Communication

Structural Roles of Boron and Silicon in the CaO-SiO_2-B_2O_3 Glasses Using FTIR, Raman, and NMR Spectroscopy

YONGQI SUN and ZUOTAI ZHANG

The present paper provided not only a deep insight of network structures of borosilicate glasses but also a basic linkage between the network structures and the viscous flow behaviors of many borosilicate melts. The structures of a ternary system of CaO-SiO_2-B_2O_3 were characterized using Fourier transformation infrared (FTIR), Raman, and magic angular spinning nuclear magnetic resonance spectroscopy. The results of FTIR and Raman spectra complementally verified that the main Si-related units were SiO_4 tetrahedral with zero, one, two, and three bridging oxygens [Q^0(Si), Q^1(Si), Q^2(Si), and Q^3(Si)]; the added B_2O_3 leaded to an increase of Q^3(Si) at the cost of Q^0(Si) and Q^2(Si), and therefore an increasing degree of polymerization (DOP) was induced. Additionally, the ^{11}B NMR spectra demonstrated that the dominant B-related groups were BO_3 trigonal and BO_4 tetrahedral, while an increasing B_2O_3 content facilitated the existence of BO_4 tetrahedral. Moreover, there was a competitive effect between the enhanced DOP and the presence of BO_3 trigonal and BO_4 tetrahedral in the networks, which therefore resulted in a decreasing viscosity of borosilicate melts in numerous studies.

DOI: 10.1007/s11663-015-0374-2

Borosilicate-based glasses and melts are important materials because of their wide applications in glass industry.[1–4] and metallurgical industry.[5–9] The macroscopic properties of these glasses and melts are primarily determined by the microscopic structure; thus it is of crucial importance to acquire the structural environments of boron (B) and silicon (Si) including the role and coordination conditions. Meanwhile, numerous studies[5–7, 10–17] explored the viscous flow behavior and analyzed the variation trend of the viscosities of B_2O_3-bearing melts. The foregoing investigations on the structures and viscosities of borosilicate glasses and melts could be categorized into three types.

First, many researchers[6,10–16] measured the viscosity of borosilicate melts and discovered that the viscosity remarkably or slightly decreased with increasing B_2O_3 content depending on the melt components, while the discussion on the varying viscosity was focused on the overall nature of B_2O_3 with a low-melting point. Second, recently several studies[5,7,17] investigated the viscosities of boron-bearing melts from the prospect of qualitative analysis of the melt structures using Fourier transformation infrared (FTIR) and Raman spectra. Third, because of the crucial importance of borosilicate glasses, many studies have explored the structures of borosilicate glasses[1–4] and substantial knowledge has been obtained.

As for the Si-related structures, there were five structural units of SiO_4 tetrahedral,[18–21] which could be denoted as Q^i(Si) (i = 0, 1, 2, 3, 4), where i represents the number of bridging oxygens (BO). The mole fraction of these structural units could be derived based on the deconvolutions of the Raman or magic angular spinning nuclear magnetic resonance (MAS-NMR) curves. Parkinson *et al.*[22] found that the fraction of Q^3(Si) decreased with more alkali in the borosilicate glasses using Raman and ^{29}Si MAS-NMR spectra. As for the B-related groups, the main structural units were BO_3 trigonal and BO_4 tetrahedron in the networks, the content of which could be deduced according to the Raman spectra or the ^{11}B MAS-NMR spectra. Du *et al.*[3,4] and Zhu *et al.*[23] separately investigated the nature of Na_2O-SiO_2-B_2O_3 and Bi_2O_3-SiO_2-B_2O_3 glasses using ^{11}B MAS-NMR, and found that the basic B-related structures were composed of 3 to 5 structural units.

However, there was limited quantitative analysis of the relationship between the viscous flow behaviors and the microscopic structures of the borosilicate melts. Therefore, the present study was motivated. In this study, we designed a basic ternary glass system, *i.e.*, CaO-SiO_2-B_2O_3 with the purpose of not only quantitatively identifying the structural characteristics of B and Si linkages but also discussing the variation trend of the viscosities measured in previous studies. Furthermore, to verify the structural analysis, FTIR, Raman, and ^{11}B MAS-NMR were complementally employed.

In this study, a series of CaO-SiO_2-B_2O_3 ternary samples were designed with a fixed CaO/SiO_2 mass ratio of 1.2. For the preparation of these samples, reagent purity grade chemicals of CaO (99.5 pct), SiO_2

YONGQI SUN, Ph.D Candidate, is with the Department of Energy and Resources Engineering, College of Engineering, Peking University, Beijing 100871, P.R. China. ZUOTAI ZHANG, Professor, is with the Department of Energy and Resources Engineering, College of Engineering, Peking University and also with the Beijing Key Laboratory for Solid Waste Utilization and Management, College of Engineering, Peking University, Beijing 100871, P.R. China. Contact e-mail: zuotaizhang@pku.edu.cn
Manuscript submitted February 4, 2015.
Article published online May 27, 2015.

Table I. Chemical Composition of Pre-melted Samples (Mass Percent)

Sample	CaO	SiO_2	B_2O_3	Basicity
CSB1	0.55	0.45	0.00	1.20
CSB2	0.52	0.43	0.05	1.20
CSB3	0.49	0.41	0.10	1.20
CSB4	0.46	0.39	0.15	1.20

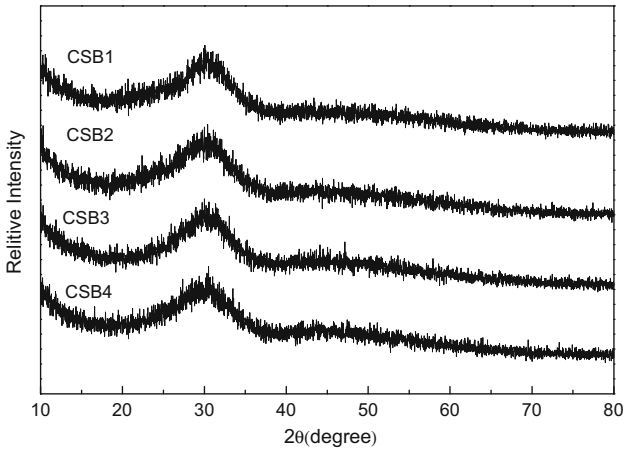

Fig. 1—XRD results of the pre-melted samples.

(99.5 pct), and H_3BO_3 (99.5 pct) (produced by Alfa Aesar company) were used. These oxides were first thoroughly mixed and placed in a Pt crucible ($\Phi 40 \times 45 \times H40$ mm), and the mixture was then pre-melted in a tube furnace at 1773 K (1500 °C) under Ar atmosphere for 2 hours to homogenize its chemical compositions. After pre-melting, the liquid melts were quickly poured into cold water and quenched to obtain a glassy state. Subsequently, the samples were dried in air at 378 K (105 °C), crushed and ground to 300 meshes. Table I shows the nominal chemical compositions of the prepared samples. To confirm the glassy nature of all samples, X-ray diffraction (XRD, D/Max 2500, Rigaku) measurement was performed, as presented in Figure 1, indicating that no crystal was precipitated.

The structures of the obtained glassy samples were characterized using various techniques including FTIR, Raman, and NMR spectra. The modes of structural group vibrations in a molecule could be Raman-active, IR-active, or both, and these two techniques were therefore complementarily employed in order to verify the structural analysis. The FTIR measurement was conducted by a spectrophotometer (Tensor 27, Bruker), equipped with a KBr detector, and the spectra were recorded in the range of 4000 to 400 cm^{-1} with a resolution of 2 cm^{-1}. As for the Raman tests, a laser confocal Raman spectrometer (JY-HR800, Jobin–Yvon Company) was operated with an excitation wavelength of 532 nm and an light source of a 1 mW semiconductor. To further identify the structural roles of B in the glasses, solid state ^{11}B MAS-NMR measures were performed using a 400M FT-NMR spectrometer (Avance III 400M, Bruker) with a MAS probe of a 4 mm ZrO_2 rotor and two pairs of Dupont Vespel caps.

As aforementioned, numerous studies investigated the viscous flow behaviors of borosilicate melts and found that an increasing B_2O_3 content generally leaded to a decreasing viscosity.[5–7, 10–17] Table II summarized these boron-bearing systems, differing from the simple ternary system of Na_2O-SiO_2-B_2O_3[10] to the complex system of CaO-SiO_2-MgO-Al_2O_3-TiO_2-B_2O_3.[7,16] Generally, a decreasing melt viscosity could be related to smaller activation energy for viscous flow or further a decrease of degree of polymerization (DOP) of the structures. Therefore, the structural characteristics of the borosilicate melts including the variation trend of the DOP and the specific structural units in the networks were clarified in this study using a series of spectroscopic techniques.

Conventionally, FTIR and Raman spectra were quite complementary to obtain the structure of glasses, as shown in Figure 2. As can be observed, the overall variation trend of FTIR spectra was similar to that of Raman spectra. First, the clarification of the binary CaO-SiO_2 glass (CSB1) would be helpful in understanding the effect of B_2O_3 on the structure of ternary CaO-SiO_2-B_2O_3 glasses. The FTIR spectra for sample CSB1 could be divided into three band regions, two weak bands of 400 to 600 and 600 to 780 cm^{-1} and a strong band of higher wavenumbers (>800 cm^{-1}), which could be assigned to O-Si-O bending vibration, Si-O symmetry stretching vibration, and stretching vibration of SiO_4 tetrahedral, respectively.[24,25] Correspondingly, the Raman spectra of CSB1 were also composed of three bands attributed to the foregoing three Si-related structures, whereas the exact locations were different, namely 300 to 580, 580 to 770, and 770 to 1150 cm^{-1}, respectively.[18–21]

As for the FTIR spectra (Figure 2(a)), the samples with B_2O_3 presented analogous trends despite the differences in the compositions. First, with increasing B_2O_3 content, the band near 680 cm^{-1} assigned to Si-O symmetry stretching became less intense due to the decreasing SiO_2 content; meanwhile, a new band attributed to the oxygen bridges between two BO_3 grew near 720 cm^{-1}.[26,27] Second, the band of Q^0(Si) centered near 840 cm^{-1} became less pronounced. This generally indicated a decreasing mole fraction of Q^0(Si) in the SiO_4 tetrahedrons and therefore an increasing DOP of the structures, which would be further discussed based on the Raman spectra. Moreover, two bands located at 1160 to 1325 and 1325 to 1550 cm^{-1} became more profound in the presence of B_2O_3, which could be attributed to the pyroborate/orthorborate units and the B-O vibrations of various borate rings, respectively.[26–28] In particular, there existed two bands centered at ~1230 and ~1410 cm^{-1}, which could be assigned to the stretching vibrations of BO_4 tetrahedral and BO_3 trigonal.[26,27] In addition, the appearance of these two B-related structures could be further verified based on the Raman and NMR spectra.

As for the Raman spectra (Figure 2(b)), the addition of B_2O_3 showed a remarkable influence on the network structures of the glasses. First, the bands associated to

Table II. Viscosities of Boron-Bearing Melt in the Previous Studies

No	Slag System	Viscosity Variation	Temperature Region	References
1	Na_2O-SiO_2-B_2O_3	decrease from 17.5 pct B_2O_3 to 35 pct B_2O_3	307 K to 927 K (580 °C to 1200 °C)	[10]
2	PbO-SiO_2-B_2O_3	decrease in the range of 17.5 to 21 pct and 0 to 100 pct B_2O_3	207 K to 607 K (480 °C to 880 °C); 577 K (850 °C)	[6,10]
3	SrO-SiO_2-B_2O_3	decrease from 5 pct B_2O_3 to 70 pct B_2O_3	343 K to 453 K (616 °C to 727 °C)	[11]
4	CaO-SiO_2-Al_2O_3-B_2O_3	decrease from 0 B_2O_3 to 10 pct B_2O_3	1087 K to 1247 K (1360 °C to 1520 °C)	[12]
5	CaO-Al_2O_3-Na_2O-B_2O_3	decrease from 10 pct B_2O_3 to 20 pct B_2O_3	1127 K to 1327 K (1400 °C to 1500 °C)	[5]
6	CaO-SiO_2-MgO-Al_2O_3-B_2O_3	decrease from 0 B_2O_3 to 4 pct B_2O_3	967 K to 1177 K (1240 °C to 1450 °C)	[13]
7	SiO_2-Al_2O_3-K_2O-Na_2O-B_2O_3	decrease from 0 B_2O_3 to 9 pct B_2O_3	327 K to 1327 K (600 °C to 1600 °C)	[14]
8	CaO-SiO_2-MgO-Al_2O_3-Na_2O-B_2O_3	decrease from 1.5 pct B_2O_3 to 8 pct B_2O_3	587 K to 1067 K (860 °C to 1340 °C)	[15]
9	CaO-SiO_2-MgO-Al_2O_3-TiO_2-B_2O_3	decrease in the range of 0 to 4.5 pct and 1 to 5 pct B_2O_3	1047 K to 1227 K (1320 °C to 1500 °C); 1067 K to 1237 K (1340 °C to 1510 °C)	[7,16]
10	CaO-SiO_2-MgO-Al_2O_3-Na_2O-TiO_2-B_2O_3	decrease from 0 B_2O_3 to 10 pct B_2O_3	747 K to 1057 K (1020 °C to 1330 °C)	[17]

Fig. 2—FTIR and Raman spectra of the glasses: (*a*) FTIR and (*b*) Raman.

O-Si-O bending[20,21] became less pronounced due to the decreasing SiO_2 content at a fixed CaO/SiO_2 ratio. Second, the band around 580 to 770 cm^{-1} was more prominent than that in FTIR spectra, which suggested that the Raman spectroscopy was very effective in probing the signal of Si-O symmetry stretching.[19–21] Third, the 860 cm^{-1} band remarkably decayed with increasing B_2O_3 content, coupled with the enhancing development of a band near 1040 cm^{-1}. These two bands could be assigned to the Q^0(Si) and Q^3(Si),[18–21] respectively, the variation of which agreed with the Raman spectra and indicated a higher DOP. Fourth, two bands centered at 1200 and 1430 cm^{-1} became more apparent with increasing B_2O_3 content, which originated from the stretching of BO_3 trigonal and BO_4 tetrahedral, respectively.[26,27,29]

To quantitatively identify the silicate structure, deconvolution of the Raman spectra was performed in the range of 770 to 1150 cm^{-1}, which was mainly attributed to the stretching vibration of Q^i(Si). Generally, the bands at ~870, ~960, ~990, and ~1050 cm^{-1} could be assigned to Q^0(Si), Q^1(Si), Q^2(Si), and Q^3(Si),[18–21] respectively, which were, therefore, employed to deconvolute the Raman curves. The fitting results of various

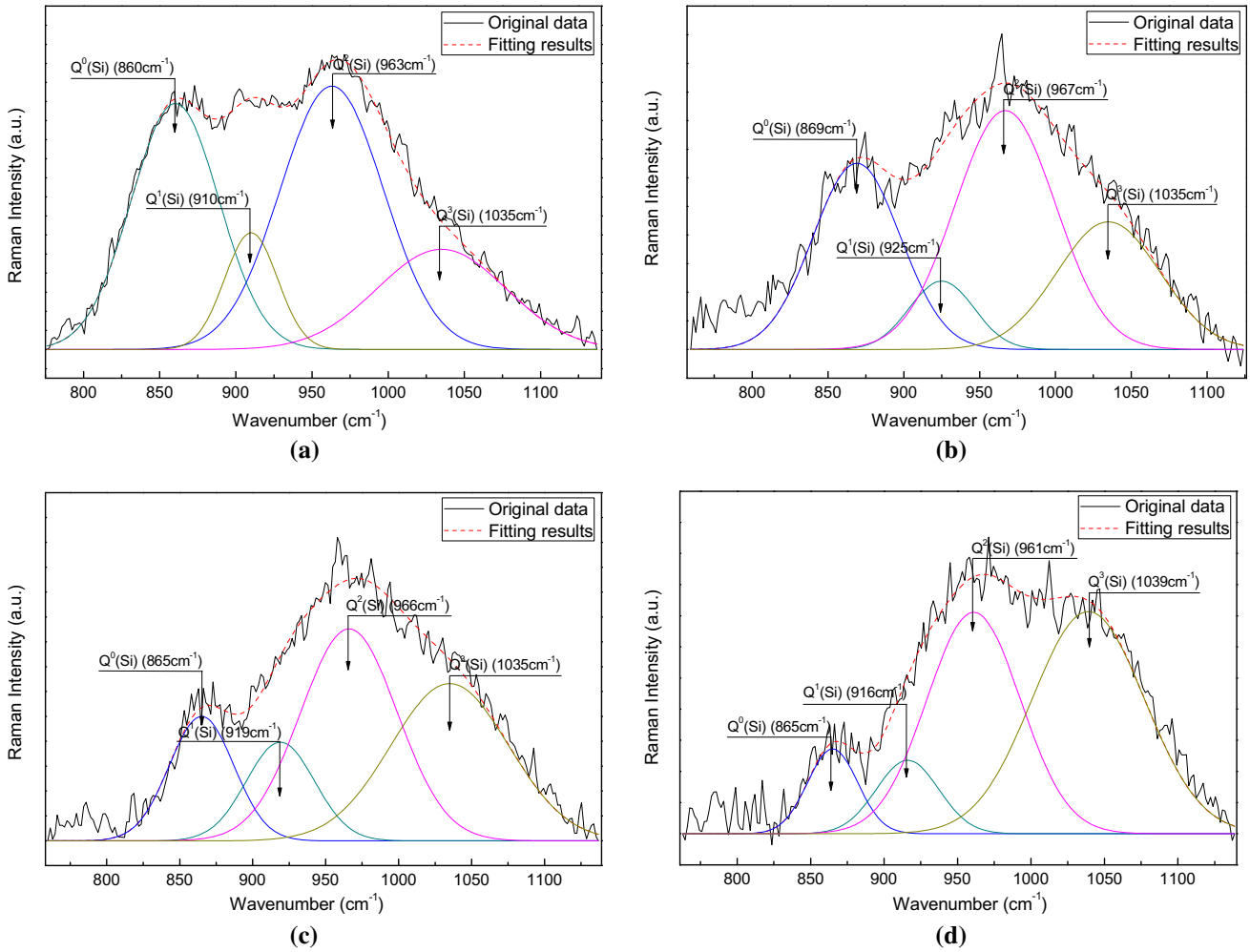

Fig. 3—Deconvolution of the Raman spectra: (*a*) CSB1, (*b*) CSB2, (*c*) CSB3, and (*d*) CSB4.

Raman curves are presented in Figure 3. Based on the areas of the obtained peaks (A_i) and the Raman scattering coefficient (S_i), the mole fractions (X_i) (i = 0, 1, 2, 3) could be calculated by Eq. [1]:[19,30,31]

$$X_i = (A_i/S_i)/\left(\sum_{i=0}^{3} A_i/S_i\right), \qquad [1]$$

where S_0, S_1, S_2, and S_3 equaled to 1, 0.514, 0.242, and 0.09, respectively.

As plotted in Figure 4, the mole fractions of Q^3(Si) considerably increased at the cost of SiO_4 tetrahedral with more non-bridging oxygens, especially Q^0(Si) and Q^2(Si), with increasing B_2O_3 content, which was in agreement with a recent study by Kline *et al.*[32] This indicated that the added B_2O_3 gave rise to a higher DOP of the networks, as also verified by the FTIR spectra. Thus it can be further concluded that the added B_2O_3 acted as a typical network former in the present glasses. Assuming that all the oxygens originally existed as bridging oxygens in the pure B_2O_3 of glassy state (B-O-B), as the B_2O_3 was introduced into the networks of silicate, it could capture the oxygens of Q^0(Si) and Q^2(Si), and therefore more Q^3(Si) was formed. In addition to Si-O-Si, the bridging oxygens could also exist in terms of Si-O-B structures in the networks;[2–4] thus it was reasonable to employ Eqs. [2] and [3] to describe the foregoing processes:

$$2\text{Si-O}^- + \text{B-O-B} \rightarrow \text{Si-O-Si} + 2\text{B-O}^- \qquad [2]$$

$$\text{Si-O}^- + \text{B-O-B} \rightarrow \text{Si-O-B} + \text{B-O}^-. \qquad [3]$$

Generally, an increase of DOP could result in an increasing viscosity of the silicate melts, which was inconsistent with the previous researches on the borosilicate melt viscosity.[5–7,10–17] Therefore, despite of DOP change, there must exist other competitive effects, which would be further discussed based on results of ^{11}B MAS-NMR spectra, as presented in Figure 5. As can be noted, the NMR spectra could be divided into two regions overall. The relatively broad region in the range of 23 to 3.7 ppm was assigned to BO_3 trigonal, and the narrow peak from −9.5 to 3.7 ppm originated from the BO_4 tetrahedral vibrations.[2–4] With increasing B_2O_3 content, the peak of BO_4 tetrahedral became more pronounced while the band of

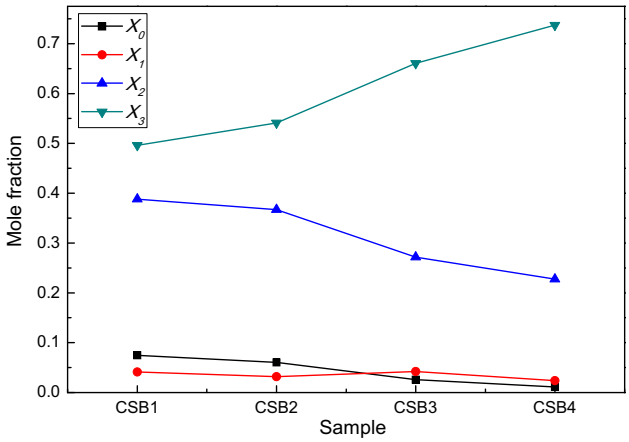

Fig. 4—Mole fractions of various Q^i(Si) units in the networks.

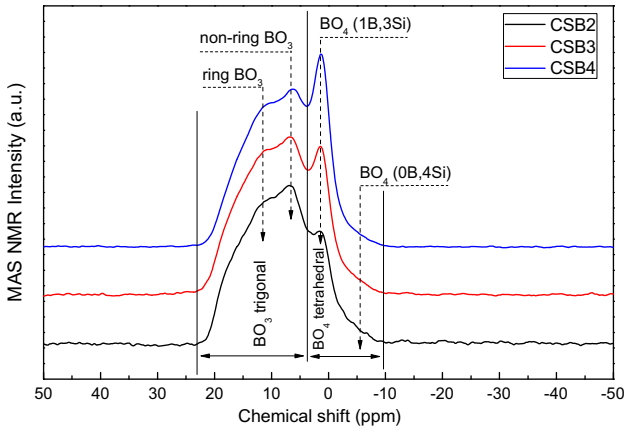

Fig. 5—^{11}B MAS-NMR spectra of the glasses.

BO_3 trigonal slightly decayed. The opposite variation trend of these two B-related coordination indicated that there was an equilibrium reaction between BO_3 trigonal and BO_4 tetrahedral, described by means of Eq. [4]. The NMR spectra undoubtedly demonstrated the existence of BO_3 trigonal and BO_4 tetrahedral in the glasses, which agreed well with the results of FTIR and Raman measurements:

$$BO_3 + 2Si\text{-}O^- \rightarrow BO_4 + Si\text{-}O\text{-}Si. \quad [4]$$

Moreover, the specific structural units associated with B atom could be identified based on the NMR spectra. BO_3 trigonal in the networks could be divided into ring BO_3 in boroxol sites and non-ring BO_3, which were located at 11.5 and 6.6 ppm in the NMR spectra, respectively.[2–4,33] As for the BO_4 tetrahedral, there existed a strong peak centered at 1.4 ppm, which was generally associated with the BO_4 tetrahedral linked with 1 B atom and 3 Si atoms (BO_4(1B,3Si)). In addition, a weak shoulder at around −5.5 ppm indicated the presence of BO_4 tetrahedral connected to 4 Si atoms (BO_4(0B,4Si)). There was an important effect named BO_4 group avoidance in the borosilicate glasses.[2,4] The BO_4 tetrahedral showed a strong preference for connection with near Si atoms with less B–B linkages formed, which was in great agreement with the observations in this study (Eq. [3]).

It is well known that the macroscopic properties are primarily determined by the microscopic structure. Thus based on the structural information obtained in this study, it could be identified more reasonably about the variation trend of the viscous flow behavior in many borosilicate melts.[5–7,10–17]

On the one hand, the increasing DOP caused by B_2O_3 addition could generally result in an increment of melt viscosity. On the other hand, with increasing B_2O_3 content, the minimum structural units that participated in the viscous flow process greatly changed, as demonstrated by the spectral results. As one of the dominant B-related units, BO_3 trigonal showed a simple two-dimensional (2D) structure, which could greatly reduce the symmetry and therefore the strength of the networks. In addition, the present BO_4 tetrahedral was preferentially connected to near Si atoms and introduced into the silicate networks because of the effect of BO_4 group avoidance; thus the uniformity of the networks could be lowered followed by a lower strength of the whole structures. In contrary to the effect of DOP increase, the existence of BO_3 trigonal and BO_4 tetrahedral greatly reduced the resistance of viscous flow process and therefore caused a more preponderant effect on decreasing the viscosity of the melts. It is thus not surprising that a decreasing slag viscosity was conventionally detected with increasing B_2O_3 content in the borosilicate melts in the previous studies.

This study explored the structures of a basic ternary system of CaO-SiO_2-B_2O_3 using FTIR, Raman, and ^{11}B MAS-NMR spectra, and the Si-related and B-related structural units were identified in the networks. It was found that the fraction of Q^3(Si) increased at the cost of Q^0(Si) and Q^2(Si), and the DOP of the glasses was therefore enhanced with increasing B_2O_3 content. The existence of BO_3 trigonal and BO_4 tetrahedral was evidently observed in the networks; in addition, the former one was composed of ring and non-ring BO_3, while the latter one could be divided into BO_4(1B,3Si) and BO_4(0B,4Si). Moreover, the present observations provided important clues of a good understanding of the viscous flow behaviors of borosilicate melts in view of network structures.

The authors gratefully acknowledge financial support by the Common Development Fund of Beijing, the National Natural Science Foundation of China (51172001, 51074009 and 51172003), the National High Technology Research and Development Program of China (863 Program, 2012AA06A114), and the Key Projects in the National Science & Technology Pillar Program (2011BAB03B02 and 2011BAB02B05).

REFERENCES

1. C. Holbrook, S. Chakraborty, S. Ravindren, P. Boolchand, J.T. Goldstein, and C.E. Stutz: *J. Chem. Phys.*, 2014, vol. 140, pp. 144506–12.
2. X. Wu, R.E. Youngman, and R. Dieckmann: *J. Non Cryst. Solids*, 2013, vol. 378, pp. 168–76.
3. L.S. Du and J.F. Stebbins: *J. Phys. Chem. B*, 2003, vol. 107, pp. 10063–76.
4. L.S. Du and J.F. Stebbins: *J. Non Cryst. Solids*, 2003, vol. 315, pp. 239–55.
5. G.H. Kim and I. Sohn: *Metall. Mater. Trans. B*, 2014, vol. 45B, pp. 86–95.
6. S. Fujino, C. Hwang, and K. Morinaga: *J. Am. Ceram. Soc.*, 2004, vol. 87, pp. 10–16.
7. Y.Q. Sun, J.L. Liao, K. Zheng, X.D. Wang, and Z.T. Zhang: *JOM*, 2014, vol. 66, pp. 2168–75.
8. Y.Q. Sun, Z.M. Li, L.L. Liu, X.D. Wang, and Z.T. Zhang: *ISIJ Int.*, 2015, vol. 55, pp. 158–65.
9. Z. Wang, Q. Shu, and K. Chou: *ISIJ Int.*, 2011, vol. 51, pp. 1021–27.
10. A.I. Priven: *Glass Phys. Chem.*, 2001, vol. 27, pp. 360–70.
11. S.V. Stolyar, N.G. Tyurnina, Z.G. Tyurnina, and L.A. Doronina: *Glass Phys. Chem.*, 2008, vol. 34, pp. 509–11.
12. H. Wang, G. Li, Q. Dai, Y. Lei, Y. Zhao, B. Li, G. Shi, and Z. Ren: *ISIJ Int.*, 2006, vol. 46, pp. 637–40.
13. H. Wang, T. Zhang, H. Zhu, G. Li, Y. Yan, and J. Wang: *ISIJ Int.*, 2011, vol. 51, pp. 702–06.
14. D.B. Dingwell, R. Knoche, S.L. Webb, and M. Pichavant: *Am. Mineral.*, 1992, vol. 77, pp. 457–61.
15. A.B. Fox, K.C. Mills, D. Lever, C. Bezerra, C. Valadares, I. Unamuno, J.J. Laraudogoitia, and J. Gisby: *ISIJ Int.*, 2005, vol. 45, pp. 1051–58.
16. S. Ren, J. Zhang, L. Wu, W. Liu, Y. Bai, X. Xing, B. Su, and D. Kong: *ISIJ Int.*, 2012, vol. 52, pp. 984–91.
17. Z. Wang, Q. Shu, and K. Chou: *Steel Res. Int.*, 2013, vol. 84, pp. 766–76.
18. P. McMillan: *Am. Mineral.*, 1984, vol. 69, pp. 622–44.
19. J.D. Frantz and B.O. Mysen: *Chem. Geol.*, 1995, vol. 121, pp. 155–76.
20. B.O. Mysen and D.R. Neuville: *Geochim. Cosmochim. Acta*, 1995, vol. 59, pp. 325–42.
21. D.R. Neuville, D.D. Ligny, and G.S. Henderson: *Rev. Mineral. Geochem.*, 2014, vol. 78, pp. 509–41.
22. B.G. Parkinson, D. Holland, M.E. Smith, C. Larson, J. Doerr, M. Affatigato, S.A. Feller, A.P. Howes, and C.R. Scales: *J. Non Cryst. Solids*, 2008, vol. 354, pp. 1936–42.
23. X. Zhu, C. Mai, and M. Li: *J. Non Cryst. Solids*, 2014, vol. 388, pp. 55–61.
24. J.H. Park, D.J. Min, and H.S. Song: *ISIJ Int.*, 2002, vol. 42, pp. 344–51.
25. S.A. MacDonald, C.R. Schardt, D.J. Masiello, and J.H. Simmons: *J. Non Cryst. Solids*, 2000, vol. 275, pp. 72–82.
26. E.I. Kamitsos, M.A. Karakassides, and G.D. Chryssikos: *J. Phys. Chem.*, 1987, vol. 91, pp. 1073–79.
27. I.J. Hidi, G. Melinte, R. Stefan, M. Bindea, and L. Baia: *J. Raman Spectrosc.*, 2013, vol. 44, pp. 1187–94.
28. A.F.L. Almeida, D. Thomazini, I.F.D. Vasconcelos, M.A. Valente, and A.S.B. Sombra: *Int. J. Inorg. Mater.*, 2001, vol. 3, pp. 829–38.
29. R.E. Youngman and J.W. Zwanziger: *J. Phys. Chem.*, 1996, vol. 100, pp. 16720–28.
30. B.O. Mysen and J.D. Frantz: *Am. Mineral.*, 1993, vol. 78, pp. 699–709.
31. Y.Q. Wu, G.C. Jiang, J.L. You, H.Y. Hou, and H. Chen: *Acta Phys. Sin.*, 2005, vol. 54, pp. 961–66.
32. J. Kline, M. Tangstad, and G. Tranell: *Metall. Mater. Trans. B*, 2015, vol. 46B, pp. 62–73.
33. R.E. Youngman, S.T. Haubrich, J.W. Zwanziger, M.T. Janicke, and B.F. Chmelka: *Science*, 1995, vol. 269, pp. 1416–20.